THE ASTROPHYSICAL JOURNAL, 505:L95–L98, 1998 October 1

KECK SPECTROSCOPY AND NICMOS PHOTOMETRY OF A REDSHIFT $z = 5.60$ GALAXY[1]

RAY J. WEYMANN,[2,3] DANIEL STERN,[4] ANDREW BUNKER,[4] HYRON SPINRAD,[4] FREDERIC H. CHAFFEE,[5]
RODGER I. THOMPSON[6], AND LISA J. STORRIE-LOMBARDI[3]
Received 1998 July 17; accepted 1998 August 6; published 1998 August 31

ABSTRACT

We present Keck Low Resolution Imaging Spectrometer spectroscopy along with Near-Infrared Camera and Multiobject Spectrometer (NICMOS) F110W (~*J*) and F160W (~*H*) images of the galaxy HDF 4−473.0 in the Hubble Deep Field (HDF), with a detection of an emission line consistent with Lyα at a redshift of $z = 5.60$. Attention to this object as a high-redshift galaxy was first drawn by Lanzetta, Yahil, & Fernandez-Soto and appeared in their initial list of galaxies with redshifts estimated from the Wide Field Planetary Camera 2 (WFPC2) HDF photometry. It was selected by us for spectroscopic observation, along with others in the HDF, on the basis of the NICMOS F110W and F160W and WFPC2 photometry. For $H_0 = 65$ km s^{-1} Mpc^{-1} and $q_0 = 0.125$, the use of simple evolutionary models along with the F814W (~*I*), F110W, and F160W magnitudes allow us to estimate the star formation rate (~13 $M_\odot$ yr^{-1}). The colors suggest a reddening of $E(B - V) \sim 0.06$. The measured flux in the Lyα line is approximately 1.0×10^{-17} ergs cm^{-2} s^{-1}, and the rest-frame equivalent width, correcting for the absorption caused by intervening H I, is ~90 Å. The galaxy is compact and regular, but resolved, with an observed FWHM of ~0.″44. Simple evolutionary models can accurately reproduce the colors, and these models predict the Lyα flux to within a factor of 2. Using this object as a template shifted to higher redshifts, we calculate the magnitudes through the F814W and two NICMOS passbands for galaxies at redshifts $6 < z < 10$.

Subject headings: early universe — galaxies: distances and redshifts — galaxies: evolution — galaxies: formation

1. INTRODUCTION

There have recently been several programs aimed at discovering galaxies at very high redshifts, utilizing the strong effects on broadband colors arising from the Lyα forest and Lyman continuum absorption (Lanzetta, Yahil, & Fernández-Soto 1996; Madau et al. 1996; Steidel et al. 1996; Spinrad et al. 1998; Fernandez-Soto, Lanzetta, & Yahil 1998), imaging to detect Lyα emission through narrowband filters (Hu, Cowie, & McMahon 1998), Fabry-Perot imaging (Thommes et al. 1998), long-slit "serendipitous" Lyα searches (Dey et al. 1998; Hu et al. 1988), and slitless spectroscopic searches (Lanzetta 1998). The ability of the *Hubble Space Telescope* (*HST*) Near-Infrared Camera and Multiobject Spectrometer (NICMOS) (Thompson et al. 1998a) to obtain very deep images over the range 0.8–1.8 μm offers an additional tool for discovering faint high-redshift candidates. We report here the detection of the first such galaxy incorporating this NICMOS data and describe some of its properties.

2. TARGET SELECTION, NICMOS IMAGES, AND PHOTOMETRY

During the first NICMOS Camera 3 *HST* campaign in 1998 January, very deep images were taken of a portion of the Wide Field Planetary Camera 2 (WFPC2) Hubble Deep Field (HDF) chip 4 in both the F110W and F160W filters, corresponding approximately to the *J* and *H* bands. A catalog of the galaxies found on these images and a discussion of its contents is presented elsewhere (Thompson et al. 1998b). Preliminary inspection of these images revealed that the galaxy HDF 4−473 (hereafter 4−473) in the Williams et al. (1996) catalog was relatively bright in F110W and F160W, distinctly fainter in the F814W (*I*) band, and not visible in F606W (*V*). Although we were unaware of it at the time, this object had already been noted by Lanzetta et al. (1996) as a high-redshift candidate, with a photometrically estimated redshift from the F814W and F606W images of 6.8. The negative F110W−F160W (AB) NICMOS color, together with the moderately red (positive) F814W−F110W AB color, made it a very strong candidate for spectroscopic observations to confirm it as a high-redshift galaxy. Indeed, combined with its nondetection by the KPNO infrared imager (Dickinson et al. 1998), the revised photometric redshift of 5.64 by Fernández-Soto et al. (1998) is remarkably close to what we have observed spectroscopically.

To measure colors on a consistent basis, we have measured 1.″0 diameter aperture magnitudes (AB scale used throughout) and obtain values of 27.12 ± 0.19 in F814W, 26.64 ± 0.04 in F110W, and 26.86 ± 0.04 in F160W. The signal-to-noise ratio of the corresponding F606W image is less than 1, and the lower limit on the F606W−F814W color is 2.31 from Williams et al. (1996). A mosaic of $3'' \times 3''$ regions around 4−473 in these four passbands is shown in Figure 1.

3. SPECTROSCOPIC OBSERVATIONS OF 4−473

Although 4−473 is extremely faint, recent successes in detecting Lyα emission from very high redshift galaxies (Dey et

[1] Optical data presented herein were obtained at the W. M. Keck Observatory, which is operated as a scientific partnership among the California Institute of Technology, the University of California, and the National Aeronautics and Space Administration. The observatory was made possible by the generous financial support of the W. M. Keck Foundation. The near-infrared observations were obtained with the Near-Infrared Camera and Multiobject Spectrometer on the NASA/ESA *Hubble Space Telescope*, which is operated by AURA Inc., under contract with NASA.
[2] Visiting Professor, Lick Observatory, Santa Cruz, CA 95064.
[3] Observatories of the Carnegie Institution of Washington, 813 Santa Barbara Street, Pasadena, CA 91101; rjw@ociw.edu, lisa@ociw.edu.
[4] Astronomy Department, 601 Campbell Hall, University of California, Berkeley, Berkeley, CA 94720; dstern@bigz.berkeley.edu, abunker@bigz.berkeley.edu, hspinrad@bigz.berkeley.edu.
[5] W. M. Keck Observatory, 65-1120 Mamalahoa Highway, Kamuela, HI 96743; fchaffee@keck.hawaii.edu.
[6] Steward Observatory, University of Arizona, Tucson, AZ 85721; thompson@as.arizona.edu.

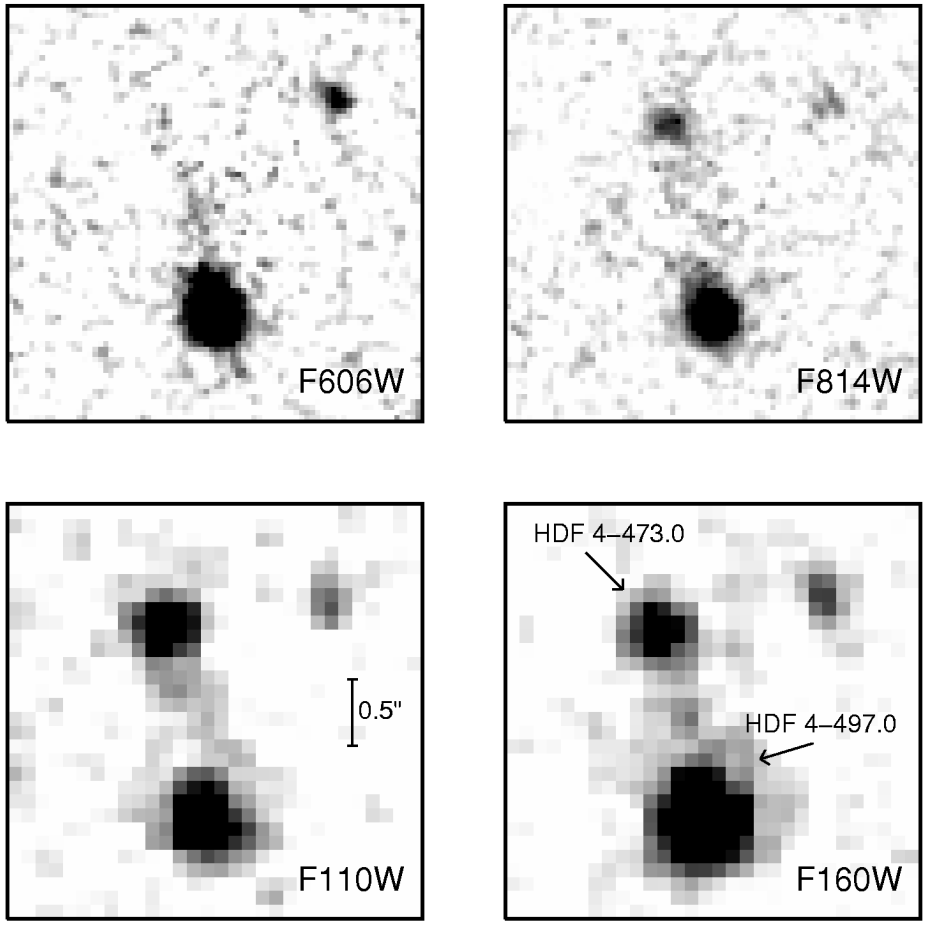

FIG. 1.—Mosaic around HDF 4−473.0 in the F606W (~*V*), F814W (~*I*), F110W (~*J*), and F160W (~*H*) passbands. AB 1″ diameter aperture magnitudes are greater than 29.4, 27.1, 26.6, and 26.9, respectively. HDF 4−473 is located at $\alpha = 12^h36^m45\overset{s}{.}902$, $\delta = 62°11'58\overset{''}{.}21$ (J2000). Images shown are 3″ on a side. Bunker et al. (1998) have shown HDF 4−497.0 to be at $z = 2.80$.

al. 1998; Hu et al. 1998) encouraged us to attempt spectroscopic observations. Accordingly, we observed the HDF on 1998 February 25 UT using the slitmask spectroscopic mode of the Low Resolution Imaging Spectrometer (LRIS) (Oke et al. 1995) at the Cassegrain focus of the Keck II Telescope. The 1″.5 wide slitlet containing 4−473 was ≈24″ long, allowing for effective sky removal. The observations were made with the 400 lines mm^{-1} grating ($\lambda_{blaze} \approx 8500$ Å; $\Delta\lambda \approx 11$ Å). The telescope was offset 2″.5 along the slit between each 1800 s exposure to facilitate removal of the fringing in the near-IR regions of the spectrogram. A total of 9000 s of integration was obtained, and the reduced spectrogram revealed a faint emission line at ≈8030 Å at the position of 4−473 on the slitlet. We therefore reobserved 4−473 for an additional 5400 s on 27 June 1998 UT with LRIS in long-slit mode, utilizing the relatively bright star HDF 4−454.0 at the center of HDF chip 4 as a control for both spectrophotometry and spectroastrometry. These observations were obtained with a 1″ slit and the 400 lines mm^{-1} grating and confirmed the emission line detected in February.

Data reductions were performed using the IRAF package and followed standard slit spectroscopy procedures. Wavelength calibration was performed using a NeAr lamp, employing telluric lines to adjust the zero point. Flux calibration employed a sensitivity function derived from 1998 January 20, 21 UT observations of G191B2B and HZ 44 (Massey et al. 1988; Massey & Gronwall 1990) and was adjusted to ensure that F814W magnitudes derived from spectrophotometry of the brighter serendipitous objects HDF 4−460.0 (1998 February data) and HDF 4−454.0 (1998 June data) matched the Williams et al. (1996) imaging photometry. Our composite spectrogram (Fig. 2) reveals a robust detection of an emission line at 8029 Å with an integrated flux of $\approx 1.0 \times 10^{-17}$ ergs cm^{-2} s^{-1}.

4. IDENTIFICATION OF THE EMISSION LINE AS Lyα

As discussed below, we believe the only reasonable identification for the emission line in 4−473 is Lyα. Other possible alternatives are Hα, [O III] λ5007, and [O II] λ3727; [O III] λ4960 or Hβ are unlikely since [O III] λ5007 would also be detected. (By chance, the slitlet for the February observations passed through the galaxy HDF 4−460.0, which has a redshift of $z \sim 0.68$ and has three lines at similar observed wavelengths as the line in 4−473.) If the line were Hα, the rest-frame colors of 4−473 would be unlike any galaxy of which we are aware. Identification of the line as [O III] λ5007 itself might be possible, since the corresponding [O III] λ4960 and Hβ lines would be weaker and in a region of strong OH night-sky emission, but the corresponding [O II] λ3727 would fall in a region uncontaminated by night-sky emission and is not present to a very low flux level. By contrast, the [O II] λ3727 line in the spectrum of HDF 4−460.0 is readily observed and is very strong.

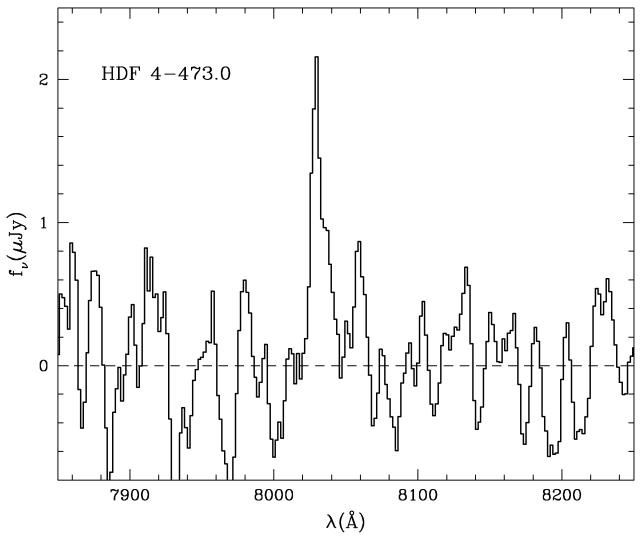

FIG. 2.—Spectrum of HDF 4−473.0 showing the emission line at 8029 Å. The asymmetric line profile and broadband colors are consistent with this being Lyα at $z = 5.60$. The total exposure time is 14,400 s, and the spectrum was extracted with a 1.″7 aperture. The spectrum has been smoothed using a 5 pixel boxcar filter.

The colors may also be used to rule out with high probability an identification as [O II] λ3727. To make this latter statement quantitative, we have used the six template spectra of star-forming galaxies assembled by Calzetti, Kinney, & Storchi-Bergmann (1994). These templates are each sets of star-forming galaxies observed both with *IUE* and from the ground and grouped into six sets characterized by different amounts of internal reddening.[7] Shifting these templates to the redshift implied if the line were identified as [O II] λ3727, the F606W−F814W colors range from 0.39 to 0.79, i.e., much *bluer* than the observed limit of greater than 2.31. Moreover, for the reddest of the templates, the F814W−F110W and F110W−F160W colors are much *redder* than the observed colors: 0.79 and 0.64 compared to the observed values of +0.48 and −0.22, respectively. Galaxies with old stellar populations, in which a hidden source of ionizing radiation might produce the [O II] λ3727 emission, encounter similar difficulties.

An additional argument in favor of the Lyα identification comes from the profile of the line itself. As seen in Figure 2, the line is asymmetric, with absorption on the blue side, just as anticipated from absorption by local H I and/or a dense Lyα forest (see Dey et al. 1998). In the following we assume, therefore, that the Lyα identification is correct, and the wavelength at the peak of the line emission implies a redshift of 5.603 ± 0.002.

5. DISCUSSION

HDF 4−473 is not the galaxy with the highest reported redshift. A galaxy of slightly higher redshift has been reported in a serendipitous long-slit exposure by Hu et al. (1998), and no doubt more high-redshift galaxies will be forthcoming from the various approaches described in § 1 (see Lanzetta 1998). However, the combination of the WFPC2 and NICMOS images allow us to make some estimates of the star formation rate as well as the reddening.

[7] We thank D. Calzetti for kindly making available these templates to us in digital form.

5.1. *Empirical Estimate of Continuum Level and Slope*

We have been unable to detect a continuum in our spectroscopic observations, since only a fairly limited portion of the spectrum redward of Lyα is free of strong OH emission. To estimate the continuum level, we use a semiempirical model in which we assume a power law of the form

$$F(\lambda) = F_0 \times (\lambda/1.6\ \mu\mathrm{m})^{\beta}$$

and impose the absorption due to the Lyα forest and Lyα continuum calculated recently by Madau, Pozzetti, & Dickinson (1998). We then determine the values of F_0 and β as well as the flux in the Lyα emission line from the F160W, F110W, and F814W magnitudes. We regard the flux in the Lyα emission line as a parameter to be determined, since our absolute flux measurement is somewhat uncertain and the Lyα flux makes a significant contribution to the total counts in the F814W filter. The magnitudes are very accurately reproduced for this redshift with $\beta = -2.40$, a Lyα flux of 1.2×10^{-17} ergs cm^{-2} s^{-1}, and a continuum flux at the Lyα line of 4.0×10^{-20} ergs cm^{-2} s^{-1} Å^{-1}. This implies a rest-frame equivalent width of about 45 Å for the unobscured portion of the line and about 90 Å if, as appears to be the case from the line profile, half of the line is absorbed away.

5.2. *Evolutionary Models, Star Formation Rate, and Reddening*

We construct evolutionary models as follows.

1. We use the latest version of the GISSEL model (Bruzual & Charlot 1993; Leitherer et al. 1996) for a Salpeter initial mass function (IMF) and 125 $M_\odot$ upper limit cutoff.
2. We use the Madau et al. (1998) Lyman absorption model.
3. We use the Calzetti et al. (1994) reddening law in which we have set the ratio R of reddening to extinction to 3.1.
4. We assume a constant rate of star formation extending from the observed epoch over some period δT yr.
5. We fix the flux of Lyα at 1.2×10^{-17} ergs cm^{-2} s^{-1} on the basis of the semiempirical determination above.
6. We adopt the cosmological parameters $H_0 = 65$ km s^{-1} Mpc^{-1} and $q_0 = 0.125$.

We have explored models in which we vary the reddening [characterized by $E(B-V)$], the rate of star formation, and the duration of the star formation epoch, δT. For a given reddening and star formation duration, we adjust the star formation rate to force agreement with the F160W magnitude. The resultant F110W−F160W and F814W−F110W colors are rather insensitive to the star formation duration, and even the inferred star formation rate is not strongly dependent upon δT over the range $20 < \delta T < 80$ Myr. We adopt in the following $\delta T = 5 \times 10^7$ yr. The F110W−F160W and F814W−F110W colors can be exactly matched with $E(B-V) = 0.06$ and a star formation rate of 13 $M_\odot$ yr^{-1}.

Estimates on the limits for the reddening and corresponding star formation rates (SFRs) are about $E(B-V) \sim 0.00$ and SFR $\sim 8\ M_\odot$ yr^{-1} and $E(B-V) \sim 0.12$ and SFR $\sim 19\ M_\odot$ yr^{-1}. These reddening and star formation rate estimates are somewhat lower than those recently obtained for galaxies at $z = 5.34$ and 4.92 by Armus et al. (1998) and Soifer et al. (1998). At a wavelength of 9900 Å, corresponding to a rest wavelength of 1500 Å, the model predicts a flux of 2.6×10^{-20} ergs cm^{-2} s^{-1} Å^{-1}. Correcting for the extinction, our adopted cosmological model implies a luminosity of 1.4×10^{41} ergs s^{-1} Å^{-1}, which

TABLE 1
PREDICTED AB MAGNITUDES FOR HIGHER REDSHIFT GALAXIES

z	Flux (Lyα)	F160W	F110W	F814W	F606W	K	F110W−F160W	F814W−F110W
5.6	1.2E−17	26.86	26.64	27.13	30.09	27.07	−0.22	+0.49
6.0	9.6E−18	26.98	26.85	27.77	32.10	27.19	−0.14	+0.92
7.0	6.3E−18	27.21	27.33	31.36	…	27.39	+0.12	+4.03
8.0	4.3E−18	27.44	27.93	…	…	27.59	+0.49	…
9.0	3.1E−18	27.63	28.63	…	…	27.76	+1.00	…
10.0	2.3E−18	27.81	29.66	…	…	27.93	+1.85	…

NOTE.—K is an AB magnitude corresponding to the K-short passband.

agrees well with the relation between star formation rate and UV luminosity proposed by Madau et al. (1998). For a cosmology with $H_0 = 50$ km s^{-1} Mpc^{-1} and $q_0 = 0.5$, the corresponding luminosity would be lower by a factor of 1.8. We do not, of course, claim that these model properties are well determined, given all the uncertainties inherent in the assumptions listed above. However, additional support comes from the *predicted* Lyα flux. If subjected to the same reddening as the continuum and if 50% is absorbed (as seems reasonable based upon the asymmetric profile), this yields a flux of 1.8×10^{-17} ergs cm^{-2} s^{-1}, in rough agreement with that observed. The modest excess in the predicted flux over our best estimate for the observed value can be ascribed to destruction by dust of the multiply scattered Lyα and/or by variations in the IMF to which the Lyα flux is moderately sensitive.

5.3. *Morphology*

Inspection of the *HST* images reveals that 4−473 has a regular, compact morphology. We note that the other $z > 5$ galaxies for which imaging exists either have multiple components (Spinrad et al. 1998) or are resolved even from the ground (Dey et al. 1998).

In F160W, the galaxy has FWHM = 0.″44. Comparison with a point-spread function (PSF) star shows that 4−473 is clearly resolved (FWHM$_{PSF}$= 0.″2) with a deconvolved half-light radius of 0.″2 (1.4 kpc), comparable to that found for many of the $z \approx 3$ Lyman-break galaxies (Giavalisco, Steidel, & Macchetto 1996). The major/minor axial ratio is measured to be $a/b = 1.15 \pm 0.04$ in F160W. Neither an exponential disk nor a de Vaucouleurs $r^{1/4}$ law fit the radial profile well. A two-component model suggests that the disk may dominate, as with other "spheroidal" objects in the HDF (Marleau & Simard 1998). The characteristic disk scale length is $r_0 \approx 2.4$ kpc.

There is a nearby brighter object, HDF 4−497.0, which Bunker et al. (1998) have shown to be a foreground system associated with the nearby Lyman-break galaxy HDF 4−555.1 (the "hot dog" at $z = 2.80$; Steidel et al. 1996). There appears to be a diffuse structure between HDF 4−497.0 and 4−473, the nature of which is uncertain. Since this feature is still visible in the F606W band, it is likely not part of the higher redshift system.

5.4. *Extrapolation to Higher Redshifts*

Using the "best-fit" model above for the star formation rate and reddening, we can then predict the magnitudes that a galaxy like 4−473 would have at higher redshifts. A more complete discussion is given in Thompson et al. (1998b). For $H_0 = 65$ km s^{-1} Mpc^{-1} and $q_0 = 0.125$ and keeping the inferred Lyα luminosity fixed, we obtain the values in Table 1. For $H_0 = 50$ km s^{-1} Mpc^{-1} and $q_0 = 0.5$, the decrease in brightness with increasing redshift is less than that for the $H_0 = 65$ and $q_0 = 0.125$ cosmology assumed in Table 1. Relative to the magnitudes in Table 1, the galaxy would be 0.04 mag brighter at $z = 6$ and 0.33 mag brighter at $z = 10$. Evidently, near-IR imaging with NICMOS is, and will continue to be, a powerful tool for the study of high-redshift galaxies out to $z \sim 10$.

The near-infrared observations are supported by NASA grant NAG5-3042 to the NICMOS instrument definition team. R. J. W. thanks the W. M. Keck Observatory and the Lick Observatory for their hospitality during the period when this work was carried out and P. McCarthy and D. Koo for useful discussions. A. B. and L. J. S. L. gratefully acknowledge financial support from NICMOS postdoctoral positions.

REFERENCES

Armus, L., Matthews, K., Neugebauer, G., & Soifer, B. T. 1998, ApJ, in press
Bruzual, G. A., & Charlot, S. 1993, ApJ, 405, 538
Bunker, A. J., Stern, D., Spinrad, H., Dey, A., Steidel, C., & Wolfe, A. 1998, in preparation
Calzetti, D., Kinney, A. L., & Storchi-Bergmann, T. 1994, ApJ, 429, 582
Dey, A., Spinrad, H., Stern, D., Graham, J. R., & Chaffee, F. H. 1998, ApJ, 498, L93
Dickinson, M. E., et al. 1998, in preparation
Fernández-Soto, A., Lanzetta, K., & Yahil, A. 1998, ApJ, submitted
Giavalisco, M., Steidel, C., & Macchetto, D. 1996, ApJ, 470, 189
Hu, E. M., Cowie, L. L., & McMahon, R. G. 1998, ApJ, 502, L99
Lanzetta, K. 1998, in Proc. Xth Rencontres de Blois, The Birth of Galaxies, Blois, France, in press
Lanzetta, K., Yahil, A., & Fernández-Soto, A. 1996, Nature, 381, 759
Leitherer, C., et al. 1996, PASP, 108, 996
Madau, P., Ferguson, H. C., Dickinson, M. E., Giavalisco, M., Steidel, C. C., & Fruchter, A. 1996, MNRAS, 283, 1388
Madau, P., Pozzetti, L., & Dickinson, M. 1998, ApJ, 498, 106
Marleau, F. R., & Simard, L. 1998, ApJ, in press
Massey, P., & Gronwall, C. 1990, ApJ, 358, 344
Massey, P., Strobel, K., Barnes, J. V., & Anderson, E. 1988, ApJ, 328, 315
Oke, J. B., et al. 1995, PASP, 107, 375
Soifer, B. T., Neugebauer, G., Franx, M., Matthews, K., & Illingworth, G. 1998, ApJ, in press
Spinrad, H., Stern, D., Bunker, A., Lanzetta, K., Yahil, A., Pascarelle, S., & Fernández-Soto, A. 1998, in preparation
Steidel, C. C., Giavalisco, M., Pettini, M., Dickinson, M., & Adelberger, K. 1996, ApJ, 462, L17
Thommes, E., Meisenheimer, K., Fockenbrock, R., Hippelein, H., Roser, H.-J., & Beckwith, S. 1998, MNRAS, 293, 6
Thompson, R. I., Rieke, M., Schneider, G., Hines, D., & Corbin, M. 1998a, ApJ, 492, L95
Thompson, R. I., et al. 1998b, in preparation
Williams, R. E., et al. 1996, AJ, 112, 1335